Electronic Supplementary Material (ESI) for Journal of Materials Chemistry C.

Supporting Information

Sticky, Thermal Tolerant, Tough BP@PVP Ionogel for Epidermal Sensors

Xiangfei Xiao[a], Haidong Zhao[a], Penji Yan[b], Hengfei Zhang[a], Xinghuan Liu[a], Xin Jia*[a] and Shuping Jin*[b, a]

[a]School of Chemistry and Chemical Engineering, Shihezi University, Shihezi 832003, People's Republic of China.

[b]College of Chemistry and Chemical Engineering, Key Laboratory of Hexi Corridor Resource Utilization of Gansu, Hexi University, Zhangye 734000, People's Republic of China.

*Corresponding author: Shuping Jin. E-mail: zjxjsp@163.com

*Corresponding author: Xin Jia. E-mail: jiaxin@shzu.edu.cn

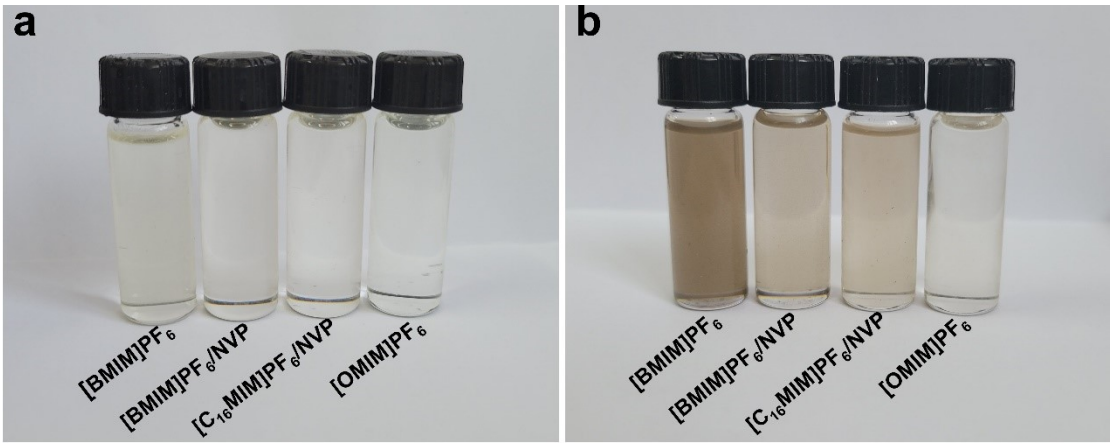

Fig. S1. (a) Photograph of the pure ionic liquids. The mass ratios of $[BMIM]PF_6$ and $[C_{16}MIM]PF_6$ to NVP are 1:1 and 1:5, respectively, for mixed solvent of $[BMIM]PF_6$/NVP and $[C_{16}MIM]PF_6$/NVP, (b) Photograph of final dispersion of BP flakes in different Ionic liquids after exfoliation, respectively. The color of the final dispersion of BP flakes in $[BMIM]PF_6$ is blackest among the other ILs dispersion, indicating that $[BMIM]PF_6$ may be an appropriate solvent for the exfoliation of BP.

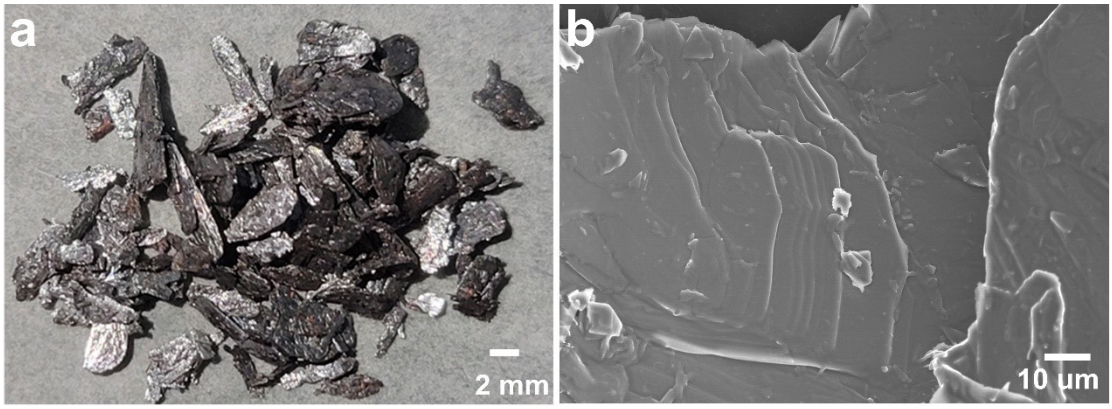

Fig. S2. (a) Photograph of Bulk black phosphorus crystals. (b) SEM image of Bulk black phosphorus suggesting the typical graphite-like vertically stacked-layer structure, of which the neighboring layers are held together weakly by the van der Waals force. [1,2]

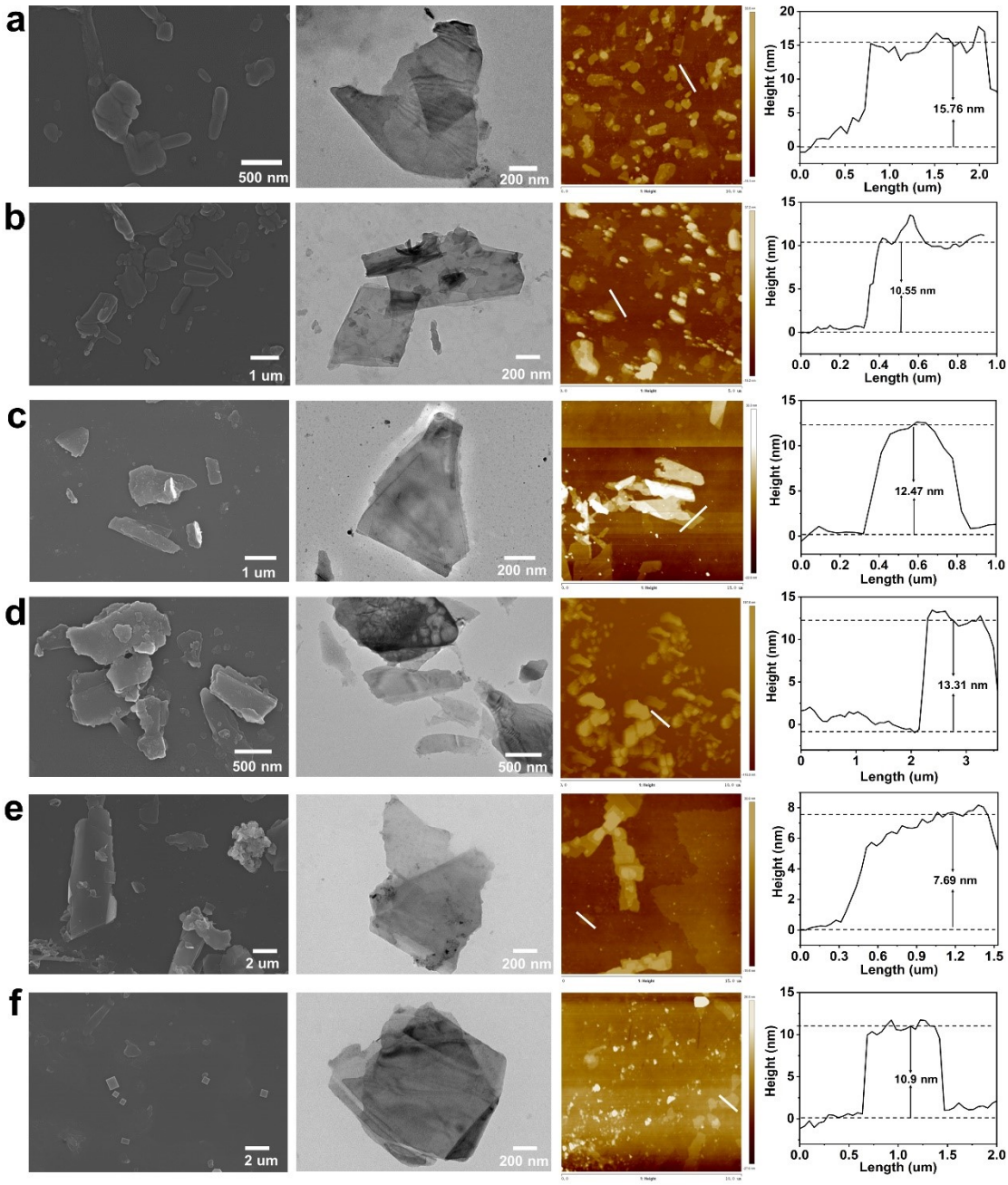

Fig. S3. SEM, TEM, AFM images and height profiles of exfoliated BP flakes in different ILs. (a) [BMIM]TF_2N, (b) [BMIM]SCN, (c) [BMIM]BF_4, (d) [BMIM]OTF, (e) [BMIM]HSO_4, (f) [BMIM]NO_3.

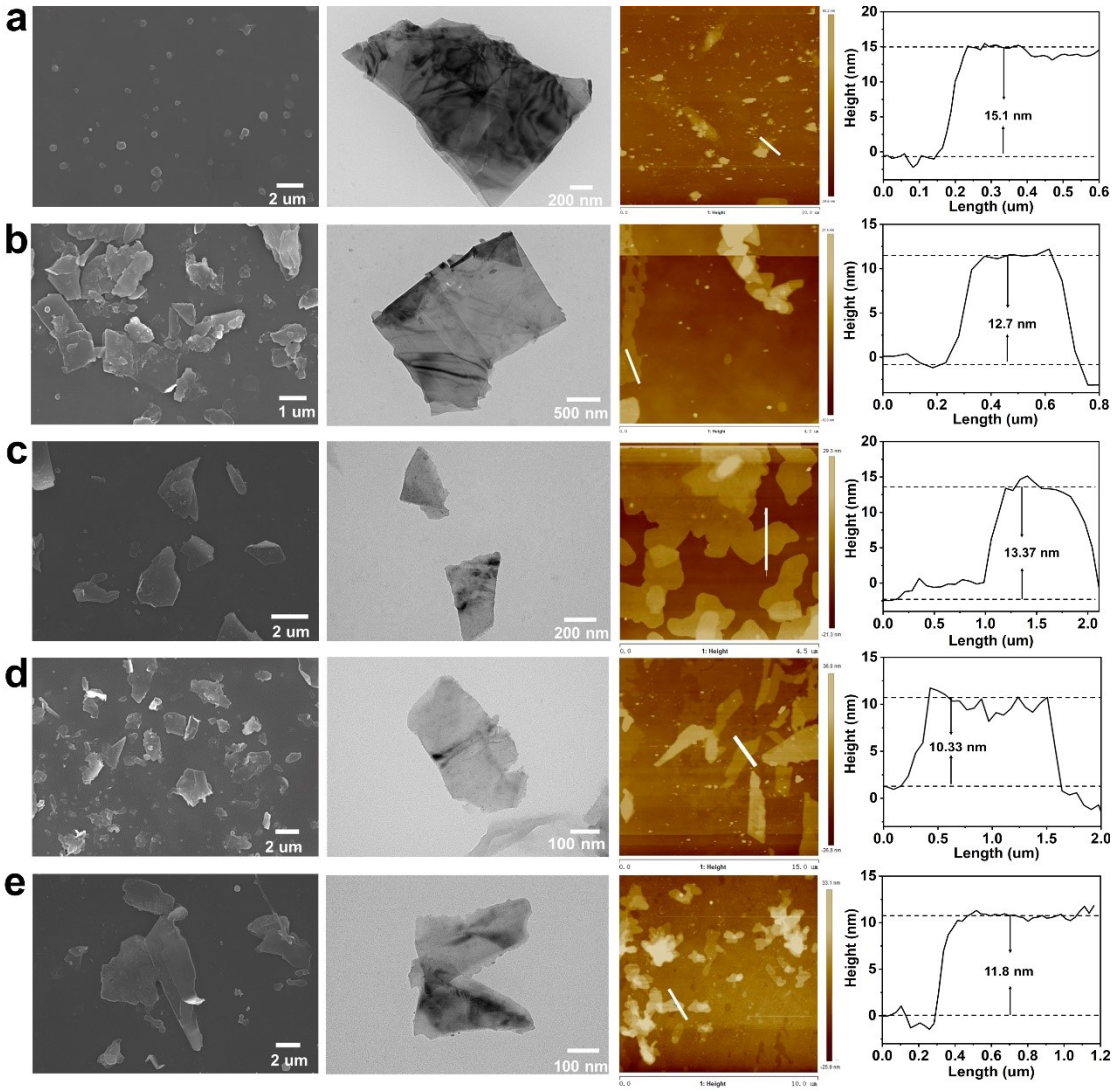

Fig. S4. SEM, TEM, AFM images and height profiles of exfoliated BP flakes in different ILs. (a) [BMIM]TFA, (b) [BMIM]I, (c) Mixed solvent [BMIM]PF_6/NVP (mass ratios of [BMIM]PF_6 to NVP is 1:1), (d) Mixed solvent [C_{16}MIM]PF_6/NVP (mass ratios of [C_{16}MIM]PF_6 to NVP is 1:5), (e) [OMIM]PF_6.

Table S1. Height, length and layer number of exfoliated BP flakes in different ILs

Solvents	Height (nm)	Length (um)	Number of layers
[BMIM]TF_2N	15.8	1.5	25-26
[BMIM]SCN	10.6	0.7	17-18
[BMIM]BF_4	12.5	0.5	20-21
[BMIM]OTF	13.3	1.8	21-22
[BMIM]PF_6	1.7	0.5	2-3
[BMIM]HSO_4	7.7	1.3	10-12
[BMIM]NO_3	10.9	0.9	17-18
[BMIM]TFA	15.1	0.4	24-25
[BMIM]I	12.7	0.6	19-20
[BMIM]PF_6/NVP	13.4	1.2	21-22
[C_{16}MIM]PF_6/NVP	10.3	1.5	16-17
[OMIM]PF_6	11.8	0.9	19-20

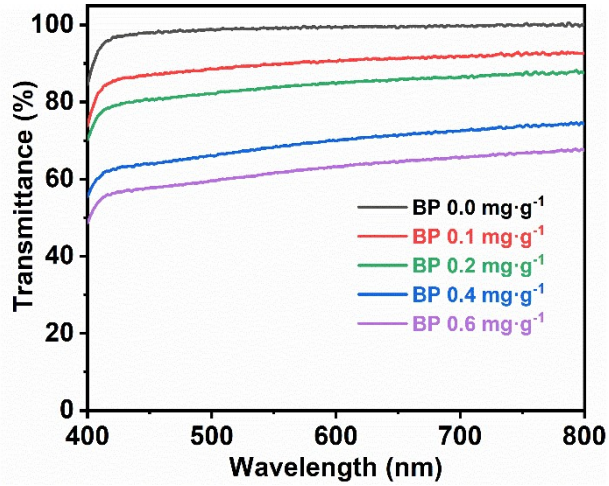

Fig. S5. The light transmittance of BP@PVP Ionogel-4555 at different BP concentrations.

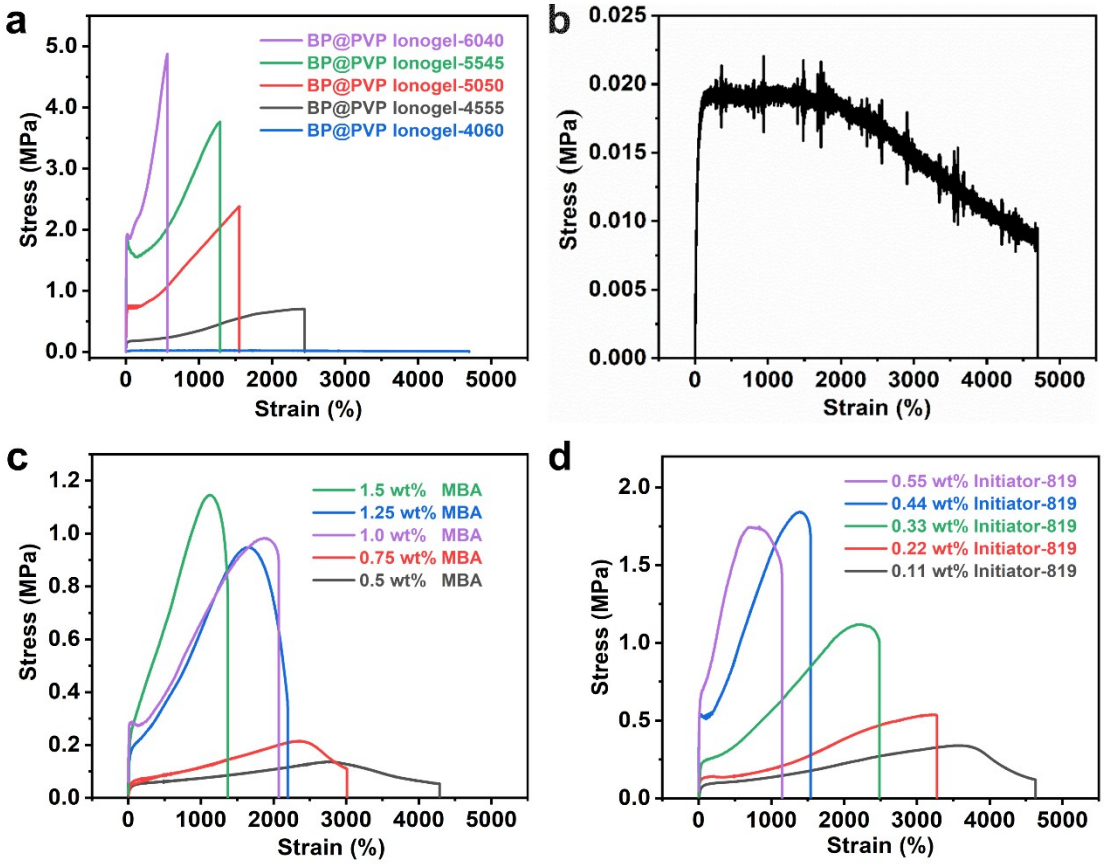

Fig. S6. Mechanical properties of the BP@PVP Ionogels obtained at 60 mm min^{-1}**.** (a) with different mass ratios of NVP to IL, (b) Mechanical properties of the BP@PVP Ionogel-4060 obtained at 60 mm min^{-1}, (c) with different mass ratios of crosslinker to NVP and (d) with different mass ratios of initiator to NVP.

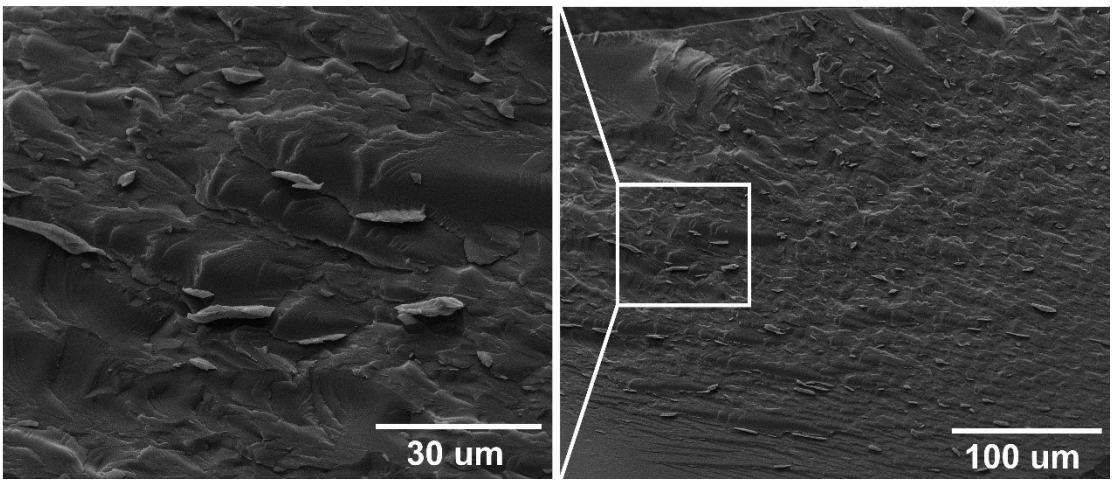

Fig. S7. Cryo-electron microscopic characterization of BP@PVP Ionogel-4555, it can be seen that the Ionogel matrix is high compact with BP flakes inlay in order indicating the strong interactions among the components of the BP@PVP Ionogel. Here, the BP flakes were used to prepare BP@PVP Ionogel without further centrifugation after being exfoliated.

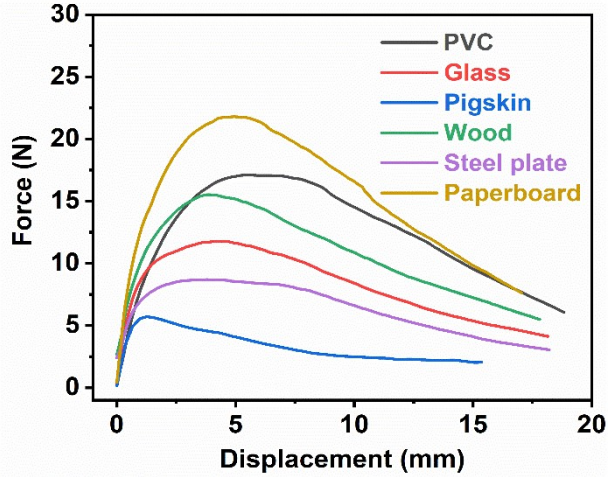

Fig. S8. Representative curves of adhesion sheer force of the BP@PVP Ionogel-4555 (20 mm × 10 mm × 1.7 mm) adhered to different substrates *vs.* displacement after storing in air without any protection for 72 h.

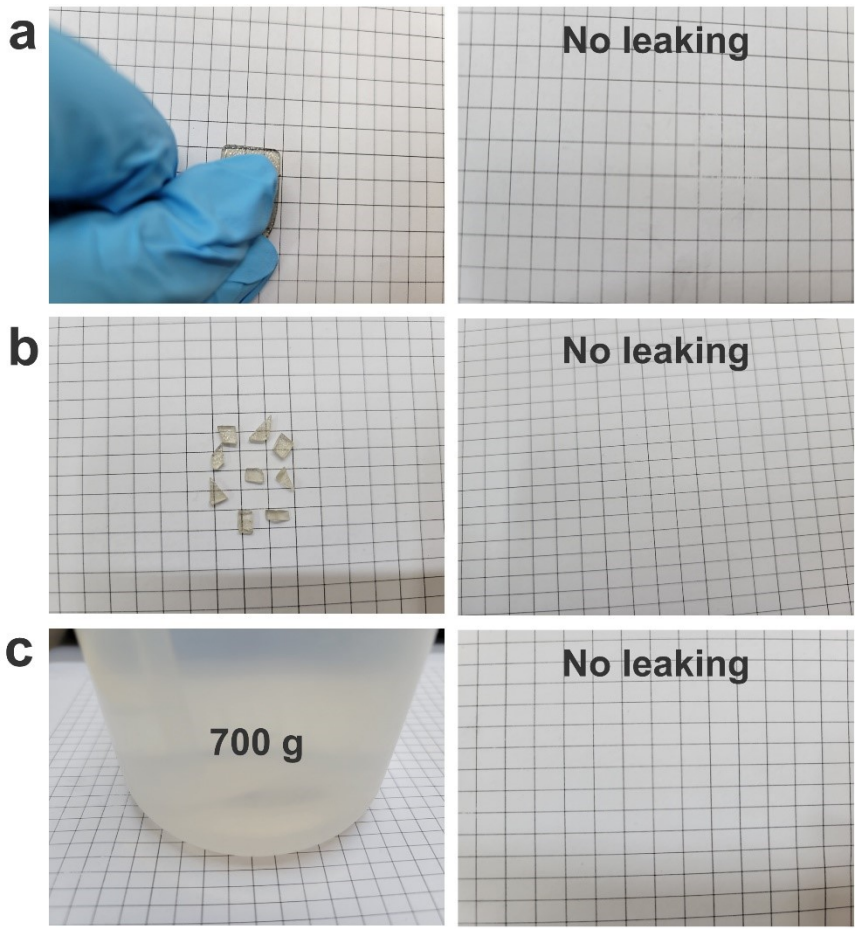

Fig. S9. Photographs of the BP@PVP Ionogel-4555 samples (a) being squeezed on plain paper, (b) chopped into pieces, and (c) under the pressure of a heavy weight (700 g). In all cases, no leaking of IL was observed.

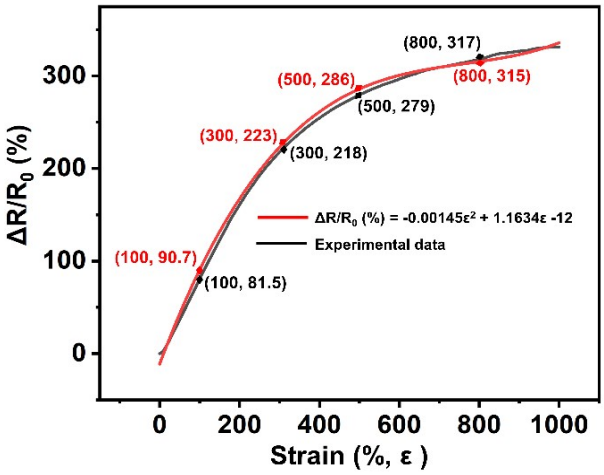

Fig. S10. Relatively resistance changes at different strains. The experimental data were compared with the theoretical prediction. The resistance of the strain sensor raised to different levels as an increase of its strain. it is observed that the experimental data matched well with the theoretical prediction.

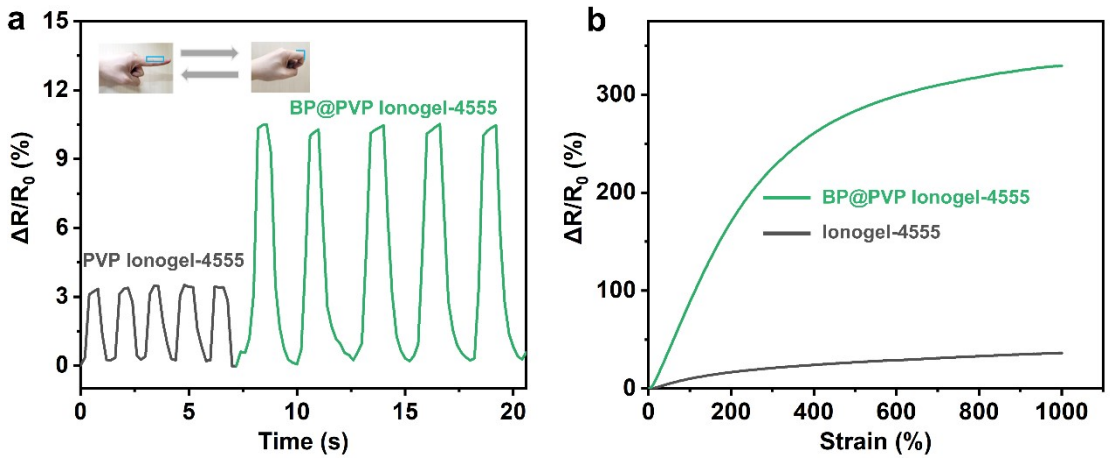

Fig. S11. Comparison of the strain sensitivity of the BP@Ionoge-4555 with the Ionogel-4555 during (a) forefinger bending to 90 degrees, and (b) sensor pulling from 0 to 1000%. It can be seen that the sensing of the BP@Ionoge-4555 ($\Delta R/R_0$ (%) = -0.000119 ε^2 + 0.098ε) with the few-layer BP nanosheets is more sensitive than the Ionoge-4555 without BP sheets. So, the BP flakes have dramatically improved sensing behavior of the BP@PVP Ionogel.

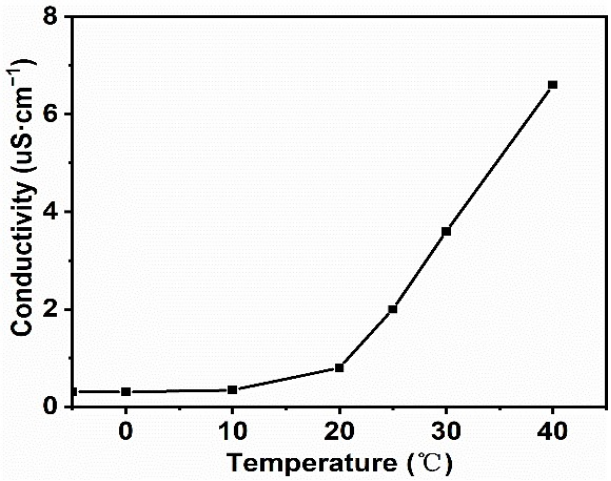

Fig. S12. The plot of the ionic conductivity of BP@PVP Ionogel-4555 versus testing temperatures ranging from -5 to 40 °C. The BP@PVP Ionogel-4555 showed increased conductivity from 3.03 $\times 10^{-4}$ mS cm^{-1} at -5 °C to 6.6$\times 10^{-3}$ mS cm^{-1} at 40 °C, owing to the more active segment movement and migration in the polymer matrix at a higher temperature.

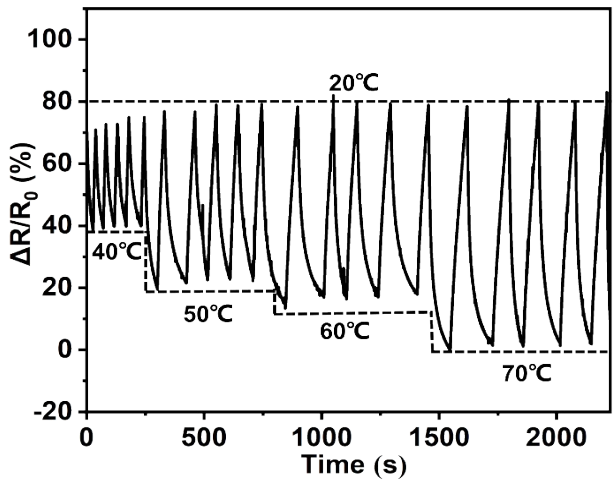

Fig. S13. Temperature sensitivity of the BP@PVP Ionogel-4555 sensor. Relative resistance changes in response to an alternating temperature change from 20 °C to 70 °C. When switching the temperature between 20 °C and 40 °C, 20 °C and 50 °C, 20 °C and 60 °C, 20 °C and 70 °C for five cycles, respectively, the $\Delta R/R_0$ keeps nearly constant demonstrating the sensitivity and good cycling stability of the BP@PVP Ionogel-4555 temperature sensor.

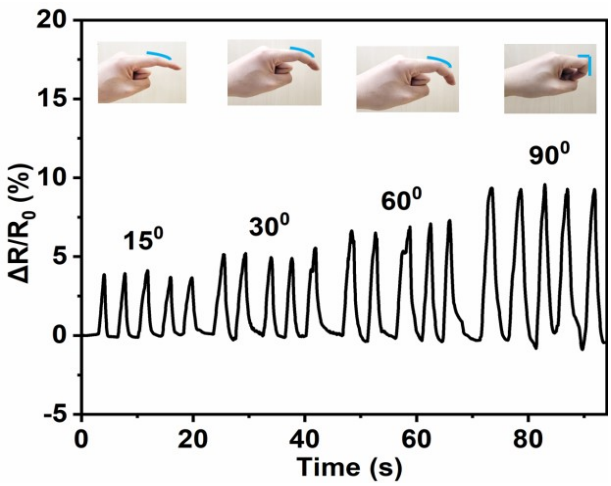

Fig. S14. Relative resistance changes of the strain sensor adhering to the forefinger to monitor its bending at different angles. Insets show the strain sensor adhering to the forefinger bending at different angles.

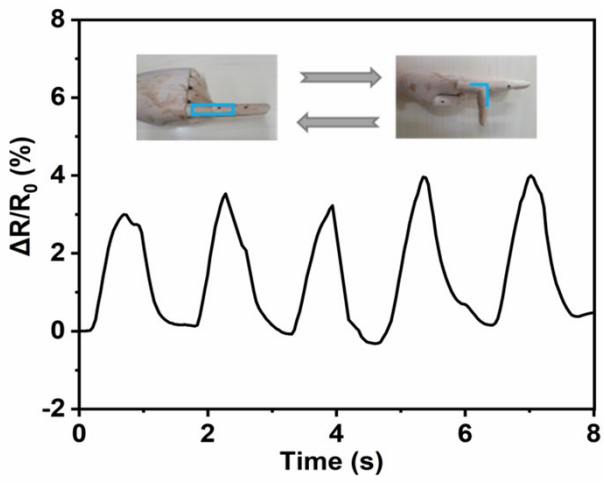

Fig. S15. Relative resistance changes of the strain sensor adhering to the forefinger of puppet to monitor its bending under -15°C environmental.

Movie 1

This movie shows sticking the BP@PVP Ionogel-4555 between two objects of different materials, making the two objects stand together, the pressure swaying, and the two objects are still firmly stuck together

Movie 2

This movie shows a video of real-time changes in the resistance of bending and straightening of the BP@PVP Ionogel-4555 fabricated sensor attached to a finger.

References

1 L. Schué, F.A. Goudreault, A. Righi, G.C. Resende, V. Lefebvre, É. Godbout, M. Tie, H.B. Ribeiro, T.F. Heinz, M.A. Pimenta, M. Côté, S. Francœur, R. Martel, Nano Letters 22 (2022) 7 2851-2858.

2 Z. Qu, K. Wu, W. Meng, B. Nan, Z. Hu, C.-a. Xu, Z. Tan, Q. Zhang, H. Meng, J. Shi, Chemical Engineering Journal 397 (2020) 125416.